

Two-dimensional electron gas at $\text{LaInO}_3/\text{BaSnO}_3$ interfaces controlled by a ferroelectric layer

Le Fang,^{1,2} Wahib Aggoune,² Wei Ren,^{1,3,*} and Claudia Draxl^{2,4,†}

¹*Materials Genome Institute, International Center for Quantum and Molecular Structures, Physics Department, Shanghai University, 200444 Shanghai, China*

²*Institut für Physik and IRIS Adlershof, Humboldt-Universität zu Berlin, 12489 Berlin, Germany*

³*Shanghai Key Laboratory of High Temperature Superconductors and State Key Laboratory of Advanced Special Steel, Shanghai University, Shanghai 200444, China*

⁴*European Theoretical Spectroscopic Facility (ETSF)*

(Dated: January 17, 2022)

With the example of $\text{LaInO}_3/\text{BaSnO}_3$, we demonstrate how both density and distribution of a two-dimensional electron gas (2DEG) formed at the interface between these perovskite oxides, can be efficiently controlled by a ferroelectric functional material. A polarization induced in a BaTiO_3 layer pointing toward the interface enhances the polar discontinuity which, in turn, significantly increases the 2DEG density and confinement, while, the opposite polarization depletes the 2DEG. Our predictions and analysis, based on first-principles calculations, can serve as a guide for designing such material combinations to be used in electronic devices.

A two-dimensional electron gas (2DEG) at the interface between two oxide perovskites was first observed at the combination of the polar material LaAlO_3 and the nonpolar compound SrTiO_3 [1]. In such a combination, electronic reconstruction occurs to compensate the polar discontinuity at the $(\text{LaO})^+ / (\text{TiO}_2)^0$ interface, forming a 2DEG within the SrTiO_3 side [2]. The latter can reach a free charge-carrier density of $\sim 3.3 \times 10^{14} \text{ cm}^{-2}$ (0.5 electrons per unit-cell area) [3] and can be confined within a few nanometers, offering the possibility to fabricate nanoscale electronic circuits in a narrow conducting path ($\sim 2 \text{ nm}$) [4, 5]. As such, 2DEGs at oxide interfaces have attracted tremendous interest due to their enormous potential in the next generation of electronic devices.

Practical applications of such interfaces, *e.g.*, in field-effect transistors (FET), require to control the 2DEG. To tune the 2DEG properties in terms of density and confinement, several external stimuli have been proposed, such as light illumination [6], strain [7], or an electric field [5, 8]. Also, addition of a functional ferroelectric layer has been suggested that allows for switching its polarization [9, 10]. Such a method can be quite effective as the microstructure of the interface itself is preserved. Indeed, a tunable 2DEG has been observed experimentally in a heterostructure consisting of $\text{LaAlO}_3/\text{SrTiO}_3$ and a ferroelectric $\text{Pb}(\text{Zr},\text{Ti})\text{O}_3$ layer [9]. Depending on the polarization direction, the 2DEG could be reversibly turned *on* and *off* with a large *on/off* ratio (>1000) in a non-volatile manner. X-ray photoelectron spectroscopy and cross-sectional scanning tunneling microscopy provided evidence for the modulation being caused by changes of the interfacial electronic structure through the ferroelectric polarization [9].

In recent years, perovskite oxide interfaces have developed rapidly, but the realization of functionality at

room temperature is still challenging. The free charge-carrier mobility is a key parameter influencing the performance of any electronic device. At the $\text{LaAlO}_3/\text{SrTiO}_3$ interface, it can reach $10^4 \text{ cm}^2(\text{Vs})^{-1}$ at low temperature, but it decreases to $1 \text{ cm}^2(\text{Vs})^{-1}$ at ambient conditions [1, 11]. The intrinsic critical reason for this lies in the partially occupied Ti-3d states that exhibit low dispersion, *i.e.*, large effective electronic masses. Furthermore, scattering of electrons within these bands reduce the mobilities through electro-acoustic coupling. As a consequence, SrTiO_3 -based heterostructures have significant limitations in practical applications in electronic devices.

Cubic BaSnO_3 is attracting great interest [12, 13] due to its extraordinary high mobilities achieved at room temperature, reaching about $320 \text{ cm}^2(\text{Vs})^{-1}$ [14, 15]. This value is two orders of magnitude larger than that of SrTiO_3 [16], and even the highest ever measured in transparent conducting oxides (TCOs). The experimental realization of coherent interfaces with LaInO_3 , exhibiting proper lattice matching [17, 18], makes the $\text{LaInO}_3/\text{BaSnO}_3$ (LIO/BSO) system a most promising combination to overcome the limitations of $\text{LaAlO}_3/\text{SrTiO}_3$ [12, 19, 20]. Therefore, it is important to explore how to control its 2DEG by an external stimulus like a ferroelectric functional layer.

To do so, state-of-the-art theory can play an important role by getting insight into the mechanisms driving the formation of 2DEGs. In this Letter, we predict by first-principles calculations that the 2DEG formed at the LIO/BSO interface can be tuned by a ferroelectric material and we rationalize the microscopic mechanism behind it. We choose the tetragonal perovskite BaTiO_3 , as it exhibits a polarization oriented along the $[001]$ direction at room temperature, providing the possibility for pointing either toward or outward the interface [21]. Moreover, as this ferroelectric material is made of neutral planes *i.e.* is nonpolar in nature, it is ideally suited for studying purely the role of ferroelectricity [21] in tuning

* renwei@shu.edu.cn

† claudia.draxl@physik.hu-berlin.de

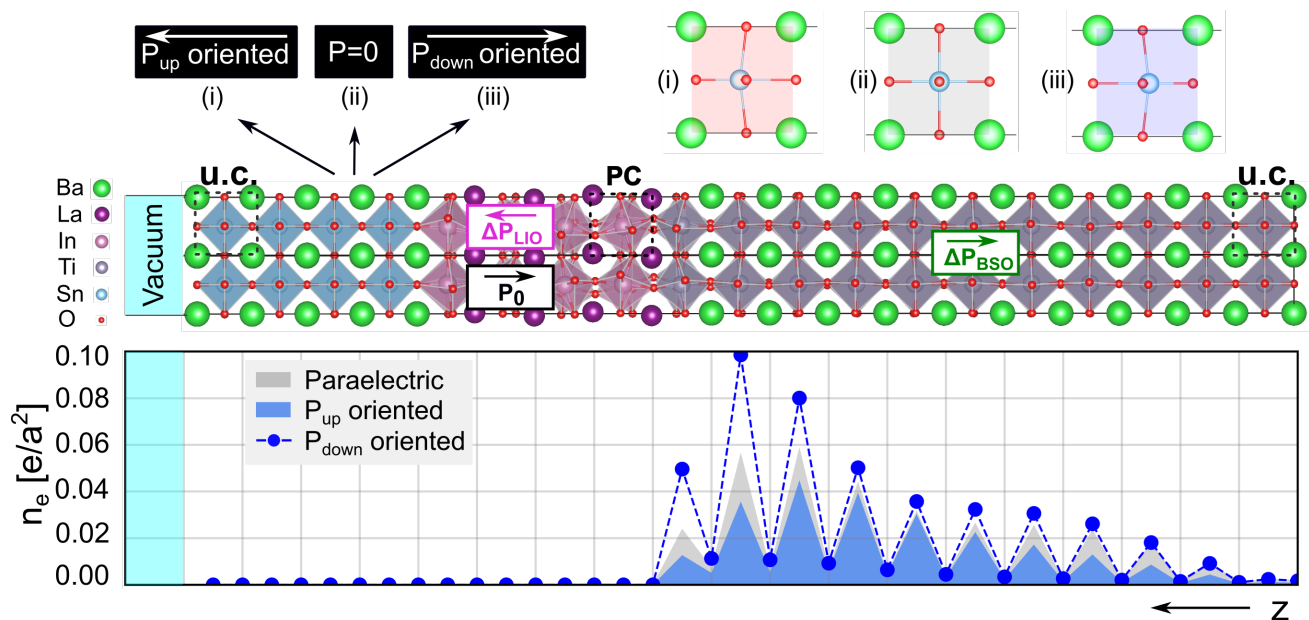


FIG. 1. Distribution of the 2D electron charge density in the BaSnO_3 side along the z direction for polarizations in BaTiO_3 oriented (i) outward (P_{up}) and (iii) toward (P_{down}) the interface, as well as the (ii) paraelectric case ($P=0$). The structural model of the BTO/LIO/BSO heterostructure is shown above. P_0 is the formal polarization oriented from the $(\text{InO}_2)^{-1}$ plane towards the $(\text{LaO})^{+1}$ plane at the interface. Polarizations due to structural distortions within LaInO_3 (ΔP_{LIO} , magenta) and BaSnO_3 (ΔP_{BSO} , green) are indicated. The BaSnO_3 and BaTiO_3 unit cells (u.c.) and the pseudocubic LaInO_3 unit cell (PC) are marked.

the 2DEG at the LIO/BSO interface. We demonstrate that switching the polarization direction allows for accumulating or depleting charge at the interface. Analyzing the so caused changes in the polar discontinuity as well as in the valence and conduction band edges, we obtain insight into the microscopic mechanism behind the formation of a controllable 2DEG at such polar/nonpolar interface. Overall, we find a gradual variation of the 2DEG density by varying the amount of polarization. We also show how the material reacts to the ferroelectric layer with structural relaxations. These predictions open possibilities for designing oxide heterostructures with tailored characteristics.

In Fig. 1, we depict the $\text{BaTiO}_3/\text{LaInO}_3/\text{BaSnO}_3$ (BTO/LIO/BSO) heterostructure, investigated in this work. The LIO/BSO interface is composed of four pseudocubic LaInO_3 and 11 BaSnO_3 unit cells, which is enough to capture the extension of the structural deformations as well as the 2DEG distribution away from the interface. The structural and electronic properties are calculated using density-functional theory (DFT) within the generalized gradient approximation (GGA) in the PBEsol parameterization [22] for exchange-correlation effects. These calculations are performed using FHI-aims [23], an all-electron full-potential package, employing numerical atom-centered orbitals. The first two BaSnO_3 unit cells are fixed to the bulk structure to simulate the bulk-like interior of the substrate. A vacuum layer (~ 140 Å) along with a dipole correction are consid-

ered in the out-of plane direction [001] in order to prevent unphysical interactions between neighboring replica. For computing the electronic properties, a $20 \times 20 \times 1$ \mathbf{k} -grid is adopted for all systems. More details related to convergence and structural relaxation for the pristine materials and their interfaces can be found in Refs. 19 and 24.

The interfacial polar discontinuity leads to the formation of a 2DEG at the BaSnO_3 side in order to compensate it. Upon increasing the LaInO_3 thickness (up to eight pseudocubic unit cells), its density increases, reaching a value of about 0.5 electrons per a^2 (a being the BaSnO_3 lattice parameter [19]). The geometry considered in this work (Fig. 1) exhibits a 2DEG density of about $0.13 e/a^2$ [19, 24]. We note that this much smaller value is not only attributed to the effect of the thickness but also to the structural distortions within the LaInO_3 block. The latter reduce the polar discontinuity, hampering the charge transfer and the formation of a high-density 2DEG [19, 24]. Such a low density is ideal for exploring how the ferroelectric overlayer can tune and enhance it.

The in-plane lattice constants of the BTO/LIO/BSO heterostructures are fixed to $\sqrt{2}a_{\text{BSO}}$, where $a_{\text{BSO}}=4.119$ Å is obtained for cubic BaSnO_3 [24]. This implies a constraint for the BaTiO_3 block whose in-plane spacing is $a_{\text{BTO}}=3.954$ Å [24]. For the BaTiO_3 bulk structure, this leads to a tetragonal distortion with a c/a ratio of 0.940 and a ferroelectric polarization of about 0.10 C/m² along the [001] direction [24], compared

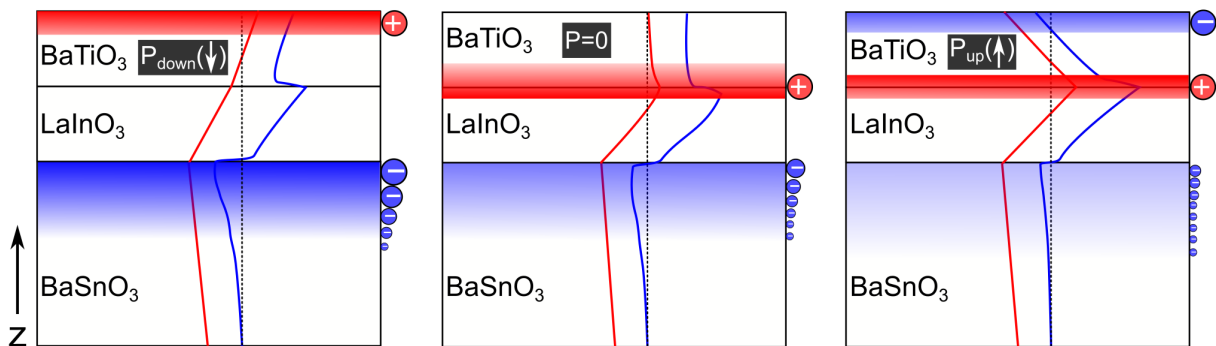


FIG. 2. Schematic diagram of the distribution of the electron and hole charges within the BTO/LIO/BSO heterostructures for P_{down} (left), $P=0$ (middle), and P_{up} polarization (right). The changes in the edges of the valence band (VBM) and conduction band (CBM), obtained from the analysis of the local density of states [24], are also highlighted. The dashed black line indicates the Fermi level.

to $c/a = 1.011$ and a polarization of 0.27 C/m^2 in the pristine material [25, 26].

The magnitude of the ferroelectric polarization reported here is estimated using the cation-anion displacements and the Born effective charges (Z^*) computed for the bulk material. The same method is used for the BaTiO_3 block within the heterostructures. Z^* are computed with the Berry-phase approach [27] using *exciting* [28], an all-electron full-potential code, implementing the family of (L)APW+LO (linearized augmented plane wave plus local orbital) methods. More details will be provided in a forthcoming publication [24].

Including a BaTiO_3 overlayer of four unit cells thickness, we select the $(\text{BaO})^0$ termination [Fig. 1 (center)] to avoid mid-gap states that would arise from TiO_2 termination [29]. Three different scenarios are considered in the BaTiO_3 block. These are (i) polarization outward of the LIO/BSO interface (termed P_{up}), (ii) the paraelectric case ($P=0$), and (iii) polarization toward the interface (termed P_{down}) [Fig. 1 (top)]. The polarization magnitude is controlled by tuning the cation-anion displacements within the BaTiO_3 block. With this approach, we mimic the experimental situations where the ferroelectric polarization (orientation and amount) is controlled by applying an electric voltage [10]. For all considered polarizations, we fix the BaTiO_3 overlayer and optimize the BaSnO_3 and LaInO_3 blocks of the BTO/LIO/BSO heterostructures. In this way, we can analyze how the 2DEG density and its distribution as well as the atomic structure at the interface react to the ferroelectric polarization and its direction.

Figure 1 depicts the distribution of the 2DEG accumulated within the BaSnO_3 block that results from the electronic reconstruction to compensate the polar discontinuity at the LIO/BSO interface [19]. For case (ii), the centrosymmetric BaTiO_3 structure, a similar 2DEG distribution is found as in the pure LIO/BSO interface, however with an increased density of up to about 0.37 e/a^2 compared to 0.13 e/a^2 in LIO/BSO. This is mainly re-

lated to the additional charge transfer from BaTiO_3 to BaSnO_3 as will be described in more detail elsewhere [24]. Analyzing the structure, we find that the presence of BaTiO_3 reduces the structural distortions within LaInO_3 (specifically in the InO_2 layer closest to BaTiO_3). This enhances the polar discontinuity at the LIO/BSO interface which, in turn, causes the increase of the 2DEG density.

Turning to the ferroelectric cases, we consider for the magnitude of both P_{up} and P_{down} , a polarization of about 0.12 C/m^2 . As the in-plane unit cells of the heterostructures are fixed to that of BaSnO_3 , the latter value is lower than the polarization in pristine BaTiO_3 ($\sim 0.29 \text{ C/m}^2$ [24]) but comparable to that of strained bulk BaTiO_3 (0.10 C/m^2 [24]). The obtained electron charge densities within the BaSnO_3 side are 0.49 e/a^2 and 0.26 e/a^2 for P_{down} and P_{up} , respectively. Comparing with the paraelectric case, we clearly see that the P_{down} case accumulates electronic charge across the LIO/BSO interface and enhances the charge density, while the P_{up} case results in charge depletion and thus a lower 2DEG density.

To get a better understanding of the mechanism behind, we analyze the band structures and the local densities of states (LDOS) of the different systems and summarize our findings in Fig. 2. For the paraelectric case, the resulting two-dimensional hole gas (2DHG) is mainly confined at the BTO/LIO interface with some extension to the BaTiO_3 layers. When we set the polarization toward the LIO/BSO interface (P_{down} case), the dipole induced within the BaTiO_3 block causes an upward shift of the valence-band edge starting from the LaInO_3 side (left panel). As such, the hole charge is enhanced and localizes at the BaTiO_3 surface rather than at the BTO/LIO interface. This result shows up in an increase of the electronic charge density within the BaSnO_3 block ($\sim 0.49 \text{ e/a}^2$). Interestingly, comparing the 2DEG distribution with the paraelectric case (Fig. 1), we find that it is more confined and accumulates near the LIO/BSO interface. Switching

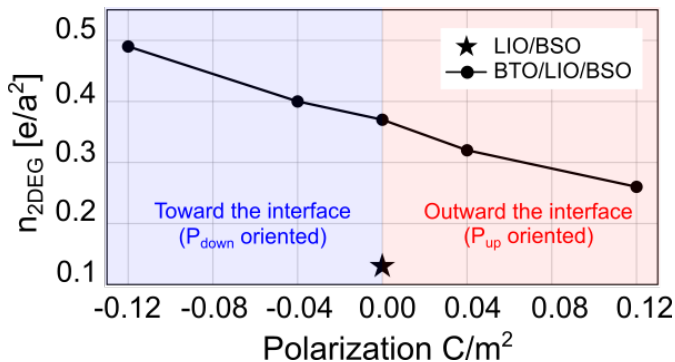


FIG. 3. Variation of the 2DEG density in the BTO/LIO/BSO heterostructure within the $BaSnO_3$ block as a function of polarization of the ferroelectric $BaTiO_3$ layer. The star refers to the 2DEG density of the pure LIO/BSO interface.

the polarization direction from the LIO/BSO interface outward (P_{up} case), induces a dipole within the $BaTiO_3$ block, but in contrast to the P_{down} case, it causes a downward shift of the valence-band edge starting from the $LaInO_3$ side of the BTO/LIO interface. Therefore, the hole charge is enhanced and localizes at the BTO/LIO interface, thereby increasing the 2DEG charge density. However, a part of the electron charge transfer is toward the $BaTiO_3$ surface to compensate its ferroelectric dipole. This process drastically reduces the 2DEG density within the $BaSnO_3$ block to about $0.26 e/a^2$ compared to that of the paraelectric case ($0.37 e/a^2$). Overall, we conclude that the ferroelectric layer with P_{up} polarization allows for depleting the 2DEG charge from the $BaSnO_3$ side.

To validate the previous findings, we vary the magnitude of the ferroelectric polarization and explore how it affects the 2DEG density within the $BaSnO_3$ block. As depicted in Fig. 3, the 2DEG charge density increases (decreases) gradually by increasing the magnitude of the ferroelectric polarization, P_{down} (P_{up}). This trend indicates that one can accumulate/deplete the 2DEG significantly [30]. Overall, the tunability of the 2DEG discussed here for the BTO/LIO/BSO combination is inline with the experimental prediction for $Pb(Zr,Ti)O_3/LaAlO_3/SrTiO_3$ [9].

Let us finally comment on the $BaTiO_3$ thickness which can also be used to tune the induced electric field. Due to the computational complexity, we have limited our calculations to four $BaTiO_3$ unit cells. To understand, nevertheless, how the thickness impacts the 2DEG density, we reduce it to three $BaTiO_3$ unit cells (details will be provided in a forthcoming publication [24]). The polarization is chosen such to achieve a similar electric field as in the previous case. We find that the 2DEG charge decreases, *i.e.*, it should conversely be enhanced with an increasing number of $BaTiO_3$ layers. All this implies that one can effectively tune the 2DEG density.

In conclusion, based on first-principles calculations, we have predicted a controllable 2DEG at the interface

between the polar $LaInO_3$ perovskite and the nonpolar $BaSnO_3$ counterpart by adding a functional ferroelectric $BaTiO_3$ layer. A polarization pointing toward the interface enhances its polar discontinuity, causing an accumulation of the 2DEG at the $BaSnO_3$ side, *i.e.*, enhancing its density. Switching the ferroelectric polarization outward of the interface depletes the 2DEG charge. Focusing on the ferroelectric side, we have found that the 2DEG density increases with its thickness. As epitaxial ferroelectric layers used experimentally are usually about tens of nanometers or more [10, 31], they are expected to give rise to a substantially higher 2DEG density. In addition, thicker layers allow for reaching higher polarization magnitudes. Moreover, we like to provide an outlook regarding other ferroelectric functional layers like $Pb(Zr,Ti)O_3$ and $(K,Na)NbO_3$. The latter offers the possibility for tuning its lattice parameter by adjusting the rate of K and Na atoms [32], thereby minimizing the lattice mismatch with the polar material. Overall, ferroelectric layers provide an effective way for controlling the characteristics of a 2DEG in terms of density and spatial distribution, which can be generalized to other heterostructures consisting of ferroelectric, polar, and non-polar components. Such heterostructures can be turned into practical applications, like in ferroelectric FETs.

DATA AVAILABILITY

Input and output files can be downloaded free of charge from the NOMAD Repository [33] at the following link: <https://dx.doi.org/10.17172/NOMAD/2022.01.11-1>.

ACKNOWLEDGMENT

L.F. and W.R. are grateful for the support from the National Natural Science Foundation of China (51861145315, 11929401, 12074241), the Independent Research and Development Project of State Key Laboratory of Advanced Special Steel, Shanghai Key Laboratory of Advanced Ferrometallurgy, Shanghai University (SKLASS 2020-Z07), the Science and Technology Commission of Shanghai Municipality (19DZ2270200, 19010500500, 20501130600), and the China Scholarship Council (CSC). This work was supported by the project BaStet (Leibniz Senatsausschuss Wettbewerb, No. K74/2017) and was performed in the framework of GraFOx, a Leibniz Science Campus, partially funded by the Leibniz Association. We acknowledge the North-German Supercomputing Alliance (HLRN) for providing HPC resources (project bep00078 and bep00096). W.A. and L.F. thank Martin Albrecht, Martina Zupancic (Leibniz-Institut für Kristallzüchtung, Berlin), Dmitrii Nabok (Humboldt-Universität zu Berlin), Chen Chen (Shanghai University) and Kookrin Char (Seoul National University) for fruitful discussions.

-
- [1] A. Ohtomo and H. Y. Hwang, *Nature* **427**, 423 (2004).
- [2] N. Nakagawa, H. Y. Hwang, and D. A. Muller, *Nat. Mater.* **5**, 204 (2006).
- [3] M. Huijben, A. Brinkman, G. Koster, G. Rijnders, H. Hilgenkamp, and D. H. A. Blank, *Adv. Mater.* **21**, 1665 (2009).
- [4] C. Cen, S. Thiel, J. Mannhart, and J. Levy, *Science* **323**, 1026 (2009).
- [5] C. Cen, S. Thiel, G. Hammerl, C. W. Schneider, K. Andersen, C. S. Hellberg, J. Mannhart, and J. Levy, *Nat. Mater.* **7**, 298 (2008).
- [6] P. Irvin, Y. Ma, D. F. Bogorin, C. Cen, C. W. Bark, C. M. Folkman, C.-B. Eom, and J. Levy, *Nat. Photonics* **4**, 849 (2010).
- [7] C. Bark, D. Felker, Y. Wang, Y. Zhang, H. Jang, C. Folkman, J. Park, S. Baek, H. Zhou, D. Fong, *et al.*, *Proc. Natl. Acad. Sci. U.S.A.* **108**, 4720 (2011).
- [8] S. Thiel, G. Hammerl, A. Schmehl, C. W. Schneider, and J. Mannhart, *Science* **313**, 1942 (2006).
- [9] V. T. Tra, J.-W. Chen, P.-C. Huang, B.-C. Huang, Y. Cao, C.-H. Yeh, H.-J. Liu, E. A. Eliseev, A. N. Morozovska, J.-Y. Lin, *et al.*, *Adv. Mater.* **25**, 3357 (2013).
- [10] S.-I. Kim, D.-H. Kim, Y. Kim, S. Y. Moon, M.-G. Kang, J. K. Choi, H. W. Jang, S. K. Kim, J.-W. Choi, S.-J. Yoon, *et al.*, *Adv. Mater.* **25**, 4612 (2013).
- [11] C. Cancellieri, A. S. Mishchenko, U. Aschauer, A. Filippetti, C. Faber, O. Barišić, V. Rogalev, T. Schmitt, N. Nagaosa, and V. N. Strocov, *Nat. Commun.* **7**, 1 (2016).
- [12] U. Kim, C. Park, T. Ha, Y. M. Kim, N. Kim, C. Ju, J. Park, J. Yu, J. H. Kim, and K. Char, *APL Mater.* **3**, 036101 (2015).
- [13] W. Aggoune, A. Eljarrat, D. Nabok, M. Zupancic, Z. Galazka, M. Albrecht, C. Koch, and C. Draxl, Preprint at <https://arxiv.org/abs/2105.07817> (2021).
- [14] H. J. Kim, U. Kim, H. M. Kim, T. H. Kim, H. S. Mun, B.-G. Jeon, K. T. Hong, W.-J. Lee, C. Ju, K. H. Kim, and K. Char, *Appl. Phys. Express* **5**, 061102 (2012).
- [15] T. R. Paudel and E. Y. Tsybal, *Phys. Rev. B* **96**, 245423 (2017).
- [16] S. Kobayashi, Y. Mizumukai, T. Ohnishi, N. Shibata, Y. Ikuhara, and T. Yamamoto, *ACS nano* **9**, 10769 (2015).
- [17] M. Zupancic, W. Aggoune, T. Markurt, Y. Kim, Y. M. Kim, K. Char, C. Draxl, and M. Albrecht, *Phys. Rev. Materials* **4**, 123605 (2020).
- [18] W. Aggoune, K. Irmscher, D. Nabok, C. Vona, S. Bin Anooz, Z. Galazka, M. Albrecht, and C. Draxl, *Phys. Rev. B* **103**, 115105 (2021).
- [19] W. Aggoune and C. Draxl, *Npj Comput. Mater.* **7**, 174 (2021).
- [20] M. Zupancic, W. Aggoune, C. Draxl, and M. Albrecht, In preparation (2022).
- [21] K. D. Fredrickson and A. A. Demkov, *Phys. Rev. B* **91**, 115126 (2015).
- [22] J. P. Perdew, A. Ruzsinszky, G. I. Csonka, O. A. Vydrov, G. E. Scuseria, L. A. Constantin, X. Zhou, and K. Burke, *Phys. Rev. Lett.* **100**, 136406 (2008).
- [23] V. Blum, R. Gehrke, F. Hanke, P. Havu, V. Havu, X. Ren, K. Reuter, and M. Scheffler, *Comput. Phys. Commun.* **180**, 2175 (2009).
- [24] L. Fang, W. Aggoune, C. Chen, C. Draxl, and W. Ren, In preparation (2022).
- [25] C. Li, D. Cui, Y. Zhou, H. Lu, Z. Chen, D. Zhang, and F. Wu, *Appl. Surf. Sci.* **136**, 173 (1998).
- [26] W. Zhong, R. King-Smith, and D. Vanderbilt, *Phys. Rev. Lett.* **72**, 3618 (1994).
- [27] R. D. King-Smith and D. Vanderbilt, *Phys. Rev. B* **47**, 1651 (1993).
- [28] A. Gulans, S. Kontur, C. Meisenbichler, D. Nabok, P. Pavone, S. Rigamonti, S. Sagmeister, U. Werner, and C. Draxl, *J. Phys. Condens. Matter.* **26**, 363202 (2014).
- [29] J. Padilla and D. Vanderbilt, *Phys. Rev. B* **56**, 1625 (1997).
- [30] More points between 0 and 0.12 C/m² without relaxation confirm the linear trend. More details will be provided in a forthcoming publication [24].
- [31] S. Wang, Y. Bai, L. Xie, C. Li, J. D. Key, D. Wu, P. Wang, and X. Pan, *ACS Appl. Mater. Interfaces* **10**, 1374 (2018).
- [32] T. Saito, T. Wada, H. Adachi, and I. Kanno, *Jpn. J. Appl. Phys.* **43**, 6627 (2004).
- [33] C. Draxl and M. Scheffler, *J. Phys. Mater.* **2**, 036001 (2019).